Biogeosciences Discuss., https://doi.org/10.5194/bg-2017-415
Manuscript under review for journal Biogeosciences
Discussion started: 1 November 2017

Biogeosciences Discussions Open Access EGU

Characterisation of aerosol provenance from the fractional solubility of Fe (Al, Ti, Mn, Co, Ni, Cu, Zn, Cd and Pb) in North Atlantic aerosols (GEOTRACES cruises GA01 and GA03) using a two stage leach

Rachel U. Shelley[1, 2, 3], William M. Landing[1], Simon J. Ussher[2], Helene Planquette[3], and Geraldine Sarthou[3]

[1]Dept. Earth, Ocean and Atmospheric Science, Florida State University, 117 N Woodward Ave, Tallahassee, Florida, 32301, USA
[2]School of Geography, Earth and Environmental Sciences, University of Plymouth, Drake Circus, Plymouth, PL4 8AA, UK
[3]Laboratoire des Sciences de l'Environnement Marin, UMR 6539 LEMAR (CNRS/UBO/IRD/IFREMER), Institut Universitaire Européen de la Mer, Technopôle Brest-Iroise, Plouzané 29280, France

Correspondence to: Rachel U. Shelley (rshelley@fsu.edu)

Abstract. The fractional solubility of aerosol-derived trace elements deposited to the ocean surface is a key parameter of many marine biogeochemical models. Yet, it is currently poorly constrained, in part due to the complex interplay between the various processes that govern the solubilisation of aerosol trace elements. In this study, we used a sequential two-stage leach to investigate the fractional solubility of a suite of aerosol trace elements (Al, Ti, Fe, Mn, Co, Ni, Cu, Zn, Cd and Pb) from samples collected during three GEOTRACES cruises to the North Atlantic Ocean. Regardless of the leaching protocol used (mild versus strong leach), the same trends were observed. These were that trace elements from aerosols from 1) North Africa were always the least soluble, and the most homogeneous (e.g. Fe was 0.36 ± 0.12 % and 6.0 ± 1.0 % soluble in North African and 6.5 ± 5.5 % and 17 ± 11 % soluble in non-African aerosols following leaches with ultra-high purity water, and 25 % acetic acid, respectively), 2) aerosols from the most remote locations were generally the most soluble, but had the most spread in the values of fractional solubility and 3) primarily pollution-derived TEs (Ni, Cu, Zn, Cd and Pb) were significantly enriched above crustal values in aerosols, even in samples of North African origin. We present aerosol trace element solubility data from two sequential leaches that provides a "solubility window", covering a conservative, lower limit to an upper limit, the maximum potentially soluble fraction, and demonstrate why this lower limit of solubility may underestimate aerosol TE solubility in some regions. The leaching technique that yields the upper limit can also be used to estimate trace element solubility from suspended particulate matter (SPM). Therefore, facilitating direct comparison with SPM leached using the same technique, thereby introducing some degree of standardisation between aerosol and SPM trace element solubility studies which may help inform of in-water processes that modify the solubility, and thus bioavailability, of atmospheric particles following deposition to the surface ocean.

Biogeosciences Discuss., https://doi.org/10.5194/bg-2017-415
Manuscript under review for journal Biogeosciences
Discussion started: 1 November 2017

1. Introduction

Aerosol trace element (TE) solubility is a key parameter of many biogeochemical models, but it is poorly constrained, e.g. Fe solubility estimates range from 0.001-90% (Aguilar-Islas et al., 2010; Baker et al., 2016). The fractional solubility (herein referred to as "solubility") of aerosol TEs is defined in terms of the amount of a TE in solution from any given leach that passes through a filter (usually < 0.45 or 0.2 µm), expressed as a percentage (Baker and Croot, 2010; Baker et al., 2016; Jickells et al., 2016). This operational definition accounts for some of the variability in published values. A number of factors impact aerosol TE solubility, such as: (1) the choice of leaching protocol, and (2) the aerosol provenance, which in turn is impacted by a combination of factors such as the mineralogy of the particles, acid processing during atmospheric transport, and the presence/absence of emissions resulting from e.g. vehicles, industry and agricultural practices. Several studies have concluded that the most significant effects on aerosol Fe solubility result from the source/composition of the aerosols, rather than changes in physico-chemical parameters, such as temperature, pH and oxygen concentration of the leach medium, or the choice of batch versus flow-through techniques (e.g. Aguilar-Islas et al., 2010; Fishwick et al., 2014).

There have been a number of studies that have focused on the role of aerosol TEs on biogeochemical cycles in the North Atlantic (e.g. Sarthou et al., 2003; Baker et al., 2013; Buck et al., 2010; Ussher et al., 2013; Powell et al., 2015). More recently, the GEOTRACES programme has produced a number of aerosol datasets, which has stimulated further discussion on the use of this data to look for trends that link TE solubility and aerosol provenance (e.g. Baker et al., 2016; Jickells et al., 2016). Elemental ratios, enrichment factors and air mass back trajectory simulations have long been used as a first approximation of aerosol source, and there are many studies that employ multivariate statistical analyses for aerosol source apportionment (e.g. Chueinta et al., 2000; Laing et al., 2015). In addition, more studies are making use of stable isotope ratios to investigate aerosol provenance. Some of these methods are well-established and have a relatively long history of use in this purpose, such as Pb isotopes (e.g. Maring et al., 1987), and Sr and Nd isotopes (e.g. Skonieczny et al., 2011; Scheuvens et al., 2013 and references therein), and data from investigations of novel isotope systems are increasing. For example, Fe isotopes show promise as a way to differentiate between anthropogenic and mineral dust aerosols (Conway et al., submitted). In contrast, Cd isotopes may not be a suitable tool for aerosol source apportionment (Bridgestock et al., 2017).

The leachable (soluble) fraction of aerosol TEs is used as a first approximation of the bioavailable fraction. Therefore, experimental conditions should mimic natural conditions as closely as possible, while yielding reproducible results. Ideally, the leach protocol used fits both these criteria. However, that is not

always strictly possible for reasons such as access to the leach medium of choice, availability of analytical instrumentation, and cost. Currently, however, there is no standardised aerosol leaching protocol, but it is recognised that this should be a priority for future studies (Baker et al., 2016). Some commonly-used leach media are ultra-high purity (UHP) water (18.2 MΩ.cm), seawater, weak acids (e.g. 1% HCl, 25 % acetic acid), or ammonium acetate buffer (e.g. Buck et al., 2006, Baker et al., 2006; Berger et al., 2008). Given that UHP water and rain water have broadly similar pH (~ pH 5.6), UHP water is used as an analogue for rain/wet deposition, as wet deposition is thought to dominate the supply of many TEs, at least at some regional and local scales (Helmers and Shremms, 1995; Kim et al., 1999; Powell et al., 2015). However, the solubilities estimated from the UHP water "instantaneous" leach (Buck et al., 2006), a flow-through method where the leach medium is in contact with the aerosols for 10 - 30 s, may be higher than those resulting from the seawater "instantaneous" leach, due to the extremely low ionic strength of UHP water. As such, freshly-collected, filtered seawater may yield more environmentally-relevant data, but can be more challenging to analyse, although analytical capabilities are rapidly improving. Nevertheless, as solubility for many TEs has been shown to be of a second order type (initial fast release, followed by a slower sustained release with time; e.g. Kocak et al., 2007; Mackey et al., 2015), the instantaneous leach likely yields conservative lower limit estimates of TE solubility due to the short contact time between the aerosols and leach medium.

In order to estimate the upper limit of TE solubility, and provide a "solubility window", a more aggressive leach is required. In this study, we have taken this approach, and estimate an upper limit of TE solubility using a leach protocol more commonly used to estimate TE solubility from suspended particulate matter (SPM; Berger at al., 2008). Therefore, a two-step, sequential leach approach was employed: (i) instantaneous UHP water leach to mimic the initial rapid release of TEs into rain drops and the surface mixed layer of the ocean, and (ii) 25 % acetic acid leach to mimic the slower and sustained release from aerosol particles during the residence time in the euphotic zone. In addition to the aerosol TE solubility data, soluble major anion (NO_3^- and non-sea salt (nss-) SO_4^{2-}) data are also discussed.

The instantaneous leach can be conducted using UHP water or sewater as the leach medium. The advantages of conducting it using UHP water are that UHP water is a reproducible medium (allowing for inter-lab comparisons), which can be easily analysed by ICP-MS for many elements simultaneously without the need for time-consuming sample handling steps such as separation techniques, and drying down and re-dissolving the residue. The UHP water leaches can easily be conducted at sea, or in the home laboratory. In addition, aliquots can be taken to determine acid species (e.g. NO_3^-, SO_4^{2-}), which can be

used to estimate aerosol acidity; an important control of aerosol metal solubility (e.g. Meskhidze et al., 2003; Solmon et al., 2009; Paris et al., 2011).

While UHP water can be thought of as an analogue for rain water (i.e. wet deposition), the extremely low ionic strength of UHP water, and the absence of the metal binding ligands naturally present in rain water and sea water (e.g. Chieze et al., 2012; Wozniak et al., 2014), means that UHP water is not a perfect analogue for oceanic receiving waters. However, freshly-collected, filtered (< 0.2 µm) sea water may be substituted for UHP water. It is assumed that the use of such water would likely produce a better estimate of the fractional solubility of TEs on first contact with the receiving waters. Despite this, sea water is a complex matrix which presents some analytical challenges, and the leaching experiments must be conducted in the field if fresh sea water is to be used. For Fe, leaches using UHP water (~ pH 5.6) typically produce higher solubility estimates than leaches conducted with natural seawater (~ pH 8.2) due to the pH sensitivity of dissolution and the higher ionic strength of sea water. On occasions where higher solubility in seawater is observed, complexation by Fe binding ligands is likely the cause. However, the short contact time between the aerosols and leaching solution during the instantaneous leach results in a conservative, lower limit of solubility, regardless of the choice of leaching medium.

In contrast, the 25 % acetic acid leach provides an upper-limit of what is potentially soluble over the life time of aerosol particles in the euphotic zone. The pH of this leach (2.1) is just below those of zooplankton or fish digestive tracts and the reducing agent mimics the low oxygen environments inside faecal pellets and marine snow aggregates. Indeed, Schmidt et al. (2016) have demonstrated that lithogenic Fe is mobilised in the gut passage of krill resulting in threefold higher Fe content in the muscle, and fivefold higher Fe content of the faecal pellets of specimens close to lithogenic source material compared to those from offshore. Use of this technique also allows direct comparison of aerosol and marine particle solubility data, which can be useful when investigating SPM provenance (e.g. terrestrial versus biogenic).

To investigate the regional variation in the solubility of key TEs in North Atlantic aerosols using the two-stage leach, samples were collected during the US-GEOTRACES GA03 campaigns in 2010 and 2011, and the French GEOTRACES GA01 campaign in 2014 (www.geotraces.org). Both campaigns took place in the North Atlantic Ocean, with GA03-2010 and GA01 departing from Lisbon, Portugal. The cruise tracks were designed to traverse a wide variety of biogeochemical provinces (Longhurst, 2010), from continental shelf regions, to an eastern boundary current upwelling system (off West Africa), the oligotrophic North Atlantic gyre, and sub-Arctic waters (North Atlantic Deep Water formation region), and span a large gradient in atmospheric dust loading. The focus of this paper is Fe and the GEOTRACES

reference elements, Al, Cd, Cu, Mn, Pb, Zn, plus Co, Ni, and Ti. This suite of TEs includes bioactive elements, tracers of atmospheric deposition, and pollutants. Some TEs fit into more than one of these categories. Here, we use the term 'trace element' in the context of open ocean water column concentrations, thus acknowledging that elements such as Al, Fe and Ti are not present in trace abundances in aerosol source material. Aerosol concentrations for a suite of other elements (Li, Na, Mg, P, Sc, V, As, Se, Rb, Sr, Sn, Sb, Cs, Ba, La, Ce, Nd, Th, U) were also determined, but will not be discussed further here. However, these data are available at BCO-DMO (GA03; www.bco-dmo.org/) and LEFE-CYBER (GA01; (www.obsvlfr.fr/proof/php/GEOVIDE/GEOVIDE.php), and on request from the lead author.

2. Methods

2.1. Aerosol sample collection

Aerosol samples (n=57) were collected in the North Atlantic Ocean aboard the *R/V Knorr* during the *US-GEOTRACES GA03* cruises (15 Oct – 2 Nov 2010 and 6 Nov – 9 Dec 2011, and aboard the *N/O Pourquoi Pas?* during the French GEOTRACES GA01 cruise (GEOVIDE, 15 May – 30 June 2014) (Fig. 1). The aerosol collections have been described previously (Wozniak et al., 2013; 2014; Shelley et al., 2015; 2017). Briefly, air was simultaneously pulled through twelve acid-washed 47 mm diameter Whatman 41 (W41) ashless filter discs at approximately 1.2 m^3 min^{-1} (134 cm s^{-1} face velocity) using a high-volume aerosol sampler (model 5170-VBL, Tisch Environmental). The metadata and concentration data for the aerosol leaches can be found in the supplementary information (Table S1). All filters were stored frozen (-20°C) and double bagged prior to processing, both on the ship and upon returning to the home laboratories.

To avoid contamination from the ship's stack exhaust, aerosol sampling was controlled with respect to wind sector and wind speed using an anemometer interfaced with a datalogger (CR800, Campbell Scientific). The samplers were programmed to run when the wind was ± 60° from the bow of the ship and > 0.5 m s^{-1}. When the wind failed to meet these two criteria, the motors were shut off automatically and not allowed to restart until the wind met both the speed and direction criteria for 5 continuous minutes. In addition, the samplers were deployed on the ship's flying bridge as high off the water as possible (~14 m above sea level) to minimise collection of sea spray.

2.2. Trace element determination – totals aerosol TEs

For the determination of total aerosol TE loadings (Al, Ti, Mn, Fe, Co, Ni, Cu, Zn, Cd, Pb) the W41 filter discs were digested in tightly-capped 15 mL Teflon-PFA vials (Savillex). Firstly, 1000 µL of ultrahigh purity (UHP) 15.8 M nitric acid (Optima or Merck ultrapur) was added to each vial, heated to 150°C on a

hotplate, and then taken to dryness. Secondly, 500 µL of 15.8 M nitric acid (13.2 M $HN0_3$) and 100 µL of 28.9 M hydrofluoric acid (5.8 M HF) (Optima or Merck ultrapur) was added to each vial, re-heated to 150°C on a hotplate, then taken to near dryness. After the final digestion and evaporation step, the samples were re-dissolved in 20 mL of 0.32 M nitric acid for analysis (Morton et al., 2013). All filter digestions were performed under Class-100 laminar flow conditions. Total aerosol TE concentrations were determined by magnetic sector field inductively coupled plasma mass spectrometry (ICP-MS; Thermo Element-2) at the National High Magnetic Field Laboratory (NHMFL) at Florida State University (FSU; GA03) or Pôle de Spectrométrie Océan (PSO) at the Institut Universitaire Européen de la Mer (IUEM; GA01), France. Samples were introduced to a PFA-ST nebuliser (Elemental Scientific Incorporated) via a modified SC-Fast introduction system consisting of an SC-2 autosampler, a six-port valve and a vacuum rinsing pump. Replicate blank solutions for the acid digestions were prepared by digesting W41 discs that had been deployed in the aerosol samplers for 1 h while not in operation, and the resulting concentrations were subtracted from all acid-digested filter samples. Details of the blanks and analytical figures of merit, including CRM recoveries, have previously been reported (Shelley et al., 2015; 2017).

2.3. Trace element determination – soluble aerosol TEs

In this study, we discuss the results from (1) an 'instantaneous' leach (Buck et al., 2006), that provides a lower limit estimate of the most labile TE fraction (analogous to the fraction that dissolves immediately on contact with water), followed by (2) a more protracted leach using 25 % acetic acid (with the reducing agent, hydroxylamine hydrochloride, and heat, 10 min at 90 °C). As this second leach aims to access a less labile fraction of the TEs of interest, without significantly attacking TEs bound within the mineral matrix (Koçak et al., 2007; Berger et al., 2008), it may provide an upper limit estimate for the fractional solubility of these aerosol TEs as the aerosols mix down into the ocean.

The "instantaneous" leach is a flow-through method using UHP water, conducted under a Class-100 laminar flow hood. Using this technique, 100 mL of UHP water (> 18 MΩ.cm resistivity, pH ~5.5, Barnstead Nanopure) is rapidly passed through an aerosol-laden W41 filter held in a polysulfone vacuum filtration assembly (Nalgene). Operationally-defined dissolved (≤ 0.45 µm) TEs are collected in the filtrate (leachate) by positioning a GN-6 Metricel backing filter (cellulose esters) below the W41 disc in the filtration assembly (Buck et al., 2006). In this study, the leachate was transferred to an acid-clean low density polyethylene (LDPE) bottle and acidified to 0.024 M (~ pH 1.7) with UHP HCl and double-bagged for storage until analysis at FSU or IUEM. As for total elemental determinations, soluble TEs in

the leachate were also determined by ICP-MS. Leachate blanks were prepared by passing 100 mL of deionised water through W41 filters that had been deployed in the aerosol sampler for 1 h. For example, leachate blanks for Fe represented an average of 1.6 ± 0.4 % and 15.5 ± 15.8 % of the Fe sample concentrations for GA03 and GA01, respectively). A subset of samples (GA03-2011) were also leached using the instantaneous leach with freshly collected, filtered (0.2 µm) seawater as the leach medium. Leachate blanks were subtracted from all leachate sample concentrations, details of which can be found in Table S1 in the Supplementary Material.

The fractional solubility was calculated using Eq. (1):

$$\frac{[element]_{leach}}{[element]_{total}} * 100 = Fractional\ Solubility \quad (1)$$

Following the instantaneous UHP water leach, the filter was transferred to a 15 mL centrifuge tube, and the second leach was undertaken, using 5 mL of 25 % (4.4 M) ultrapure acetic acid, with 0.02 M hydroxylamine hydrochloride as the reducing agent (Berger et al., 2008). After a 10 min heating step (90 °C), the leaches were left for 24 h, before being centrifuged for 5 min at maximum power (3400xg). The leachate was then carefully decanted into acid-clean LDPE bottles. In order to rinse any residual acetic acid from the filter, 5 mL of UHP water was pipetted into the centrifuge tubes, which were then centrifuged for a further 5 min on maximum power. This supernatant was then added to the relevant leachate in the LDPE sample bottles. In this study, all samples were leached first using the UHP water instantaneous leach, followed by a sequential leach with 25 % acetic acid. The overall solubility in 25% acetic acid is calculated as the sum of the UHP water and acetic acid leaches divided by the total concentration.

2.4. Major anions and aerosol acidity

Before the UHP water leachate was acidified, a 10 mL aliquot was taken from each sample leach for the determination of the soluble major anions, Cl^-, NO_3^- and SO_4^{2-}, by ion chromatography using either a Dionex 4500i (at FSU for GA03 samples) or a Metrohm, IC850 system (at Laboratoire Interunivesitaire des Systèmes Atmosphériques, Paris for GA01 samples). The aliquot was immediately frozen for storage. Non-sea salt sulfate (nss-SO_4^{2-}) was calculated using the concentration of soluble Cl^- as the reference element to correct for SO_4^{2-} from sea spray aerosols. In this study, aerosol acidity is estimated from the concentration of NO_3^- plus two times the concentration of nss-SO_4^{2-} (Buck et al., 2010).

229

230 **2.5. Aerosol source characterisation**

231 Air mass back trajectory (AMBT) simulations were generated using the publicly-available NOAA Air
232 Resources Laboratory Hybrid Single-Particle Lagrangian Integrated Trajectory (HYSPLIT) model, using
233 the GDAS meteorology (Stein et al., 2015; Rolph, 2017). The 5-day AMBT simulations were used to
234 describe five regional categories, based on the predominant trajectories for the air masses. Simulations
235 and further details of these categories can be found in Wozniak et al., (2013; 2014) and Shelley et al.,
236 (2015; 2017). Briefly, for cruise GA03 air masses were characterised as European, North American,
237 North African, or Marine (no or minimal interaction with major continental land masses within the 5-day
238 simulation period). For cruise GA01, all the samples were classified as High Latitude dust (originating
239 north of 50°N; Bullard et al., 2016). The classifications are shown in Table S1.

240

241 **3. Results and Discussion**

242 **3.1. Total aerosol TEs**

243 Atmospheric inputs to the ocean are episodic, and exhibit a seasonality in the tropical and subtropical
244 North Atlantic that is largely driven by the migration of the intertropical convergence zone (Prospero et
245 al., 1981; Adams et al., 2012; Doherty et al., 2014). North African/Saharan mineral dust dominated
246 aerosol composition in the GA03 study region (Shelley et al., 2015; Conway and John, 2015; Conway et
247 al., submitted). In contrast, the GA01 transect was located north of the extent of the Saharan dust plume
248 (~ 25° N in summer, Ben-Ami et al., 2009), and was thus influenced by different, high latitude dust
249 sources (Prospero et al., 2012; Shelley et al., 2017), which also have a seasonal cycle. As a result, a large
250 dynamic range of aerosol loading was observed (Fe = 0.185–5650 ng m^{-3}; Al = 0.761- 7490 ng m^{-3}), with
251 the highest Fe and Al loadings associated with the North African samples (GA03), lower loadings with
252 the Marine samples (GA03), and the lowest loadings observed in the samples collected in the Labrador
253 Sea (GA01). Total aerosol TE data from the GA01 and GA03 cruises have been discussed in detail
254 elsewhere (Shelley et al. 2015; 2017), the data are only discussed here for comparison.

255 For all of the GA01 and GA03 samples, total Fe and Al were strongly correlated (r^2 = 0.999, Pearson's ρ
256 $P < 0.01$), demonstrating that the two metals have common lithogenic source(s) (Fig. 2). The correlation
257 between Fe and Al was largely driven by the heavily-loaded North African dust samples (r^2 = 0.997, $P <$
258 0.01). However, with the North African samples removed, only total Fe and Al from the GA01 High
259 Latitude dust (r^2 = 0.879, $P < 0.01$) and European (r^2 = 0.890, $P < 0.05$) samples were significantly
260 correlated, and there was no correlation between Fe and Al in the samples of N. American (r^2 = 0.153, P

> 0.05) or Marine (r^2 = 0.0.16, P > 0.05) provenance (Fig. 2b) Looking more closely at the data, two of the European samples (n = 4) have anomalously low Fe/Al ratios (Fig. 2; E3 = 0.48, E4 = 0.10), compared to the other two samples of European origin (E1 = 0.95 and E2 = 0.78), and compared to the North American samples, which are also thought to be strongly influenced by anthropogenic emissions (Fe/Al 1.1 ± 0.22, range 0.86-1.42).

Strong correlations for the combined data set including all samples were found between Ti/Al (r^2 = 0.999, P < 0.01), Mn/Al (r^2 = 0.994, P < 0.01) and Co/Al (r^2 = 0.996, P < 0.01), in accord with previous observations in this region owing to the primarily lithogenic source of these elements (e.g. Jickells et al., 2016). The correlations between Al and the primarily anthropogenic TEs, Ni, Cu, Zn, Cd, and Pb, were also significant at the 99% confidence level (Pearson's ρ): Ni/Al (r^2 = 0.884), Cu/Al (r^2 = 0.652), Pb/Al (r^2 = 0.478), Zn/Al (r^2 = 0.321), Cd/Al (r^2 = 0.303) and the fraction of the statistical variance accounted for by the heavily-loaded North African samples ranges from 88% for Ni to 30% for Cd. Sources other than mineral dust (e.g. metal smelting emissions, fly ash, vehicle emissions, volcanic ash, proglacial till) are presumably responsible for the residual variance.

We have previously reported a mass ratio of 0.76 for Fe/Al for the North African end-member aerosols (Shelley et al., 2015; Fig. 2a), which is significantly higher than the mean upper continental crustal (UCC) ratio of 0.47 (Rudnick and Gao, 2003), suggesting that the North African aerosols were relatively depleted in Al compared to Fe and other elements. Elemental mass ratios greater than the UCC ratio have previously been observed for Saharan soils and dust (e.g. Guieu et al., 2002; Baker et al., 2013).While there is evidence for anthropogenic source(s) of aerosol Fe to the North Atlantic (Fig. 2b), which has an impact on aerosol Fe solubility (Sedwick et al., 2007; Sholkovitz et al., 2009; 2012), North African mineral dust dominates the supply of Fe to much of the study region (Baker et al., 2013; Shelley et al., 2015; 2017; Conway et al., submitted). In addition to the samples of European and North American provenance, the Marine samples also show elevated Fe/Al ratios (Fig. 2b). The aerosols we classify as "Marine" contain Fe and Al which presumably originated from continental source regions, but they may also contain anthropogenic aerosols that have higher Fe/Al ratios. In addition, sea spray aerosols could make a relatively higher contribution to the bulk aerosol in remote oceanic locations (de Leeuw et al., 2014). However, this would have the opposite effect as the ratio of Fe/Al in surface seawater is two orders of magnitude lower than the crustal ratio (0.017 – 0.024 in the North Atlantic gyre, 0.019 European continental shelf, and 0.030 – 0.031 in the Mauritanian upwelling zone; Hatta et al., 2015). Hence the contribution of sea spray aerosols appears to have a negligible impact on the Fe/Al ratios in the bulk Marine aerosols.

293

294 **3.2. Elemental mass ratios and aerosol provenance**

295 Aluminium was used to normalise the aerosol loading data (Fig. 3). It was chosen instead of Ti, another
296 proxy for mineral dust, due to the presence of some anomalously high Ti/Al ratios in some of the Marine
297 samples during GA03 (Fig. 3a; Shelley et al., 2015). Due to the relative depletion of Al, relative to other
298 TEs, in the North African aerosol samples collected during GA03, the elemental ratios reported here are
299 higher than the UCC elemental ratios (Rudnick and Gao, 2003). Elemental mass ratios from the ten most
300 heavily loaded GA03 North African aerosols were averaged to derive a value for the 'North African' ratio
301 depicted by the dashed horizontal line in Figures 3(a-i). The similarity to the GA03 North African
302 aerosols, which have an Fe/Al ratio of 0.78 ± 0.03 (Fig. 3c), and the relatively small range in the ratio of
303 total Fe/Al for this same section (0.85 ± 0.20), and evidence from the stable Fe (δ^{56}Fe) fractionation in
304 seawater and the aerosol UHP water leaches (Conway and John, 2014; Conway et al., submitted) provides
305 evidence that North African mineral dust consistently dominates the supply of aerosol Fe to the tropical
306 and sub-tropical North Atlantic.

307 In contrast, aerosols from the more northerly section, GA01, were largely outside the influence of the
308 Saharan dust plume (Shelley et al., 2017), and are all classified as High Latitude (Fig. 3). During the first
309 half of the cruise (samples G1-8, Fig. 1), the Fe/Al ratios were intermediate between the UCC ratio (0.48
310 ± 0.07) and the North African mineral dust ratio (0.78 ± 0.03) for both the total and soluble fractions
311 (medians of 0.56 and 0.63, respectively). As the wind direction was predominantly from the north
312 (Shelley et al., 2017), it is unlikely that the observed ratios reflect a mixture of North African mineral dust
313 and European aerosols. Rather, it is more likely from a high latitude source, as dust supplied by proglacial
314 till from Iceland and Greenland peaks in spring/early summer, and can be deposited over the Atlantic
315 Ocean (Prospero et al., 2012; Bullard et al., 2016), although the extensive cloud cover experienced during
316 the GA01 cruise (May/June 2014) prevented the use of satellite observations (e.g.
317 http://worldview.earthdata.nasa.gov) which would have confirmed the presence of dust from this source.
318 However, the TE concentrations reported by Achterberg et al. (2013) from volcanic ash sampled during
319 the eruption of the Eyjafjallajökull volcano in 2011 offers some support for this argument, as our range of
320 elemental ratios encompasses this end-member (Icelandic soils are almost exclusively volcanic in origin;
321 Arnalds 2004), for most of the TEs, but also supports mixing with pollution-derived aerosols.

322 The most heterogeneous group of data were the samples from the most remote locations (Marine and
323 High Latitude). This was also the group with the greatest difference in the Fe/Al ratio between the total
324 and soluble fractions, and with the lowest ratios of Fe/Al in the soluble fraction (minimum Fe/Al = 0.15,

samples G9-GA01 and M3-GA03; Fig. 3c), suggesting that even though aerosol Fe is altered towards more soluble forms during atmospheric transport (Longo et al., 2016), atmospheric processing renders Al even more soluble relative to Fe. However, there is some contradiction between the information from the elemental ratios and the fractional solubility of Fe. Still using the examples of samples G9-GA01 and M3-GA03 (low Fe/Al), both samples had European air mass back trajectories (Shelley et al., 2015; 2017). However, the fractional solubility for Fe differed from 20 % for G9-GA01 to 0.8 % for M3-GA03, suggesting that the reason for this disparity is that North African mineral dust was contributing to the composition of the bulk aerosol during GA03. Recent advances in the determination of stable isotopes present a powerful tool that can now be used to test such hypotheses, and have confirmed this was the case on GA03, where there was a distinct isotopic signature associated with aerosols from Europe, and North America, that differed from North African mineral dust (Conway et al., submitted).

For the anthropogenically enriched TEs, Ni, Cu, Zn, Cd and Pb (Figs. 3e-i) and for at least some of samples of the mixed-source TEs, Mn and Co (Figs. 3b and d), there is some degree of source-dependence in the elemental ratios, with some significant increases from the UCC mass ratios in the total (Shelley et al., 2015) and UHP water soluble fractions (Fig. 3). The higher ratios of the UHP water soluble fraction compared to the total indicates that these TEs are more labile than Al, which is related to where each TE occurs on the particle (surface coatings versus matrix-bound). In addition, studies that have investigated the size distribution of aerosols have found that pollution-derived TEs tend to be associated with fine mode aerosols (< 1 µm diameter), which are more soluble than coarse mode aerosols due to the larger surface area to volume ratio (Duce et al., 1991; Baker and Jickells 2006), some fraction of which will pass through the 0.2 µm filter. Size fractionated samples were collected during the GA03 cruise, and the smaller size fractions were indeed more soluble than the larger (Landing and Shelley, 2013). Enrichment of TEs with predominantly anthropogenic sources accords with other studies in the North Atlantic, and is most striking for aerosols that did not originate from the sparsely-populated arid regions of North Africa (e.g. Buck et al., 2010; Gelado-Cabellero et al., 2012; Patey et al., 2015; Shelley et al., 2015).

In addition, positive matrix factorisation analysis suggests that aerosols from this study were dominated by two factors, a mineral dust factor and a pollution factor (Fig. S2a, Supplementary Material). Unsurprisingly, the mineral dust factor dominated where North African aerosols were sampled, and the pollution factor dominated closer to the European and North American continents (Fig. S1b). This is in accord with the samples from North Africa having elemental mass ratios that are consistently the closest to the UCC elemental ratios compared to aerosols from the other source regions (Fig. 3). In the High Latitude samples, the pollution factor and the mineral dust factor were of approximately equal dominance.

Interestingly, the North African aerosols also contained a relatively strong pollution component, consistent with a northeast flow into North Africa from Europe, followed by entrainment of mineral dust during passage over the Sahara. Given that the PMF indicates that 100 % of the variability in the Cd concentrations was explained by the pollution factor, this suggests that Cd in North African aerosols is not sourced from mineral dust, which would explain why no fractionation was observed in Cd isotopes from North African and European aerosols (Bridgestock et al., 2017). Further, it also suggests that even the relatively homogeneous aerosols of North African provenance do not represent a 'pure' end-member.

3.3. Aerosol solubility

3.3.1. Solubility of aerosol Fe and Al: UHP water (instantaneous) compared to 25 % acetic acid leaches

The UHP water soluble fraction of aerosol Fe and Al determined for all the North Atlantic GA01 and GA03 samples varied by two orders of magnitude (Fig. 4a: Fe = 0.14 - 21 %, median 2.2 %; Fig. 4c: Al = 0.34 - 28 %, median 2.7%). Although a broader range of Fe and Al solubility was observed in this study, both these results and those reported by Buck et al. (2010) using the same approach (Fe = 2.9 - 47%, median = 14%, and Al = 3.7 - 50%, median = 9.5%) broadly agree that the median UHP water soluble fractions of Fe compared to Al in the North Atlantic are similar. While there was considerable overlap in the ranges of fraction solubility of TEs in aerosols of different provenance (e.g. Fe: European 1.9 – 21 %; N. American 0.84 – 8.8 %; Marine 1.7 –18 %; High Latitude dust 1.9 – 20 %), the North African samples, identified by their orange colour, high Fe and Al loadings, and definitive air mass back trajectories) formed a distinct cluster of very poorly soluble Fe, or Al (< 1%; Fig. 4a and c). However, the solubility of the North African ('Saharan') aerosol Fe was 1 – 2 orders of magnitude lower in this study (0.14 – 0.57 %) than during the Buck et al. (2010) study (2.9 – 19 %). This supports the hypothesis that TEs from North African aerosols sampled with a higher frequency closer to source (as in this study) are less soluble as a result of a lesser degree of atmospheric processing and/or larger particle sizes (Baker and Jickells, 2006; Longo et al., 2016). Furthermore, given that the Sahara Desert is the largest source of mineral dust to the atmosphere globally (the North Atlantic Ocean receives ~ 40 % of the mineral dust inputs to the global ocean, Jickells et al., 2005), the effects of increasing industrialisation/urbanisation of African countries, coupled with large unknowns in the magnitude of future mineral dust supply, and biomass burning, the ability of models to replicate subtleties in aerosol TE solubility may prove critical in forecasting ecosystem impacts and responses. In other words, it is important to accurately constrain aerosol trace element solubility with high quality data in order to improve the predictive capacity of models.

The relationship between total aerosol Fe and the soluble fraction can be described by a hyperbolic function (Fig. 4a and b), in accord with Sholkovitz et al. (2009; 2012). The same relationship was observed for aerosol Al (Fig. 4c and d). The insets in Figure 4 plot the data on a log-log scale, and illustrate the inverse relationship between Fe or Al solubility and atmospheric loading, and demonstrates that while the absolute values for solubility are dependent on the leach media used, the general trend is maintained. Jickells et al. (2016) compiled solubility data from the North Atlantic and also found that the inverse relationship between Fe and Al solubility and atmospheric loading was robust over the range of atmospheric loadings found in the North Atlantic, regardless of the leach protocol employed.

In this study, both the UHP soluble, and 25 % acetic acid soluble fractions of Fe and Al (Figs 4a and d) were related to atmospheric loading, i.e. the highest loaded North African samples had the lowest solubility. This trend is consistent with the observations of Jickells et al. (2016). The possible exception to this trend is the fraction of Al that dissolved from North African aerosols following the 25 % acetic acid leach (Fig. 4d). However, it could simply be that we are observing scatter in our data, which is smoothed out in the larger dataset (n > 2000) examined by Jickells et al. (2016). Furthermore, the solubility range estimated for Al (0.3 – 28 % and 4.1 – 100 % solubility in UHP water and 25 % acetic acid, respectively) far exceeds the relatively narrow range used in the MADCOW model (1.5 – 5 %), which has been used to estimate atmospheric inputs based on dissolved Al concentrations in the mixed layer (Measures and Brown, 1996), even taking the more conservative UHP water-derived values (0.3 – 28 %), which has implications for the estimation of atmospheric deposition fluxes. It is noted, however, that the median values from this study fall within the range used by the MADCOW model (2.7 % and 3.3 % for UHP water and 25 % acetic acid, respectively).

Furthermore, the fractional solubility of bioactive TEs from aerosols is taken as a rough approximation of bioavailability. Yet, clearly the choice of leach media impacts the estimated value. For elements with generally low solubility, such as Fe, the difference between 1 % and 2 % solubility is an increase of 100 %, meaning that only half the amount of dust is needed to yield the same amount of dissolved Fe, the most-readily bioavailable form of Fe (Shaked and Lis, 2009). To complicate matters further, recent research has demonstrated that some diazotrophs are able to directly access particulate Fe (Rubin et al., 2011). Given that the different leaching approaches access different fractions of TEs (loosely bound to surfaces compared with associated with less reactive phases), that dissolve from aerosols at different rates (e.g. Kocak et al., 2007; Mackey et al., 2015), we need to conduct experiments that elucidate the relationship between the soluble and bioavailable fractions.

Furthermore, in productive regions where Fe (and perhaps other TEs) associated with lithogenic particles is directly available to micro-organisms (Rubin et al., 2011) or in regions where particulate Fe is processed by zooplankton (Schmidt et al., 2016), we are likely underestimating bioavailable Fe using the instantaneous approach (Buck et al., 2006). Therefore, the different leaching approaches can be used to probe specific questions related to the response of the microbial community to changes in aerosol type and/or supply by providing a "window of solubility". This is an important consideration as the true solubility of aerosol TEs in the upper ocean cannot be directly measured.

3.3.2. Solubility of TEs: UHP water (instantaneous) compared to 25 % acetic acid leaches

All ten TEs from the five different provenances were less soluble in UHP water than 25 % acetic acid (Fig. 5). This is not a surprising finding given the lower pH of acetic acid compared with UHP water, that acetate is a bidentate ligand, and the longer contact time of the aerosols with the leach solution in the 25 % acetic acid leach procedure. In addition, there is some degree of source-dependent variability in the relative proportions of each TE that is released by the two leaches. In general, as with the leaches with UHP water, the North African aerosols were distinctly less soluble than aerosols from the other source regions (Fig. 5). Figure 6 highlights the distinction between the lithogenic elements, Al, Fe and Ti (universally low solubility in UHP water, mostly < 20 %, and extremely low solubility of North African aerosols, < 1 %) and the pollution-dominated elements, Ni, Cu, Zn, Cd and Pb (solubility up to 100 %). Manganese (Mn) and Co have both lithogenic and anthropogenic sources (mixed-source), and have intermediate solubilities. Like all the TEs reported here, Mn solubility in UHP water was significantly less ($p < 0.01$, two-tailed, homoscedastic t-test) in North African aerosols (median solubility = 19 %) than in the non-North African samples (median = 38%), which seems to contrast somewhat with the findings of Baker et al. (2006) and Jickells et al. (2016). However, in common with these earlier studies (Baker et al., 2006; Jickells et al., 2016), there was no significant source-dependent difference in Mn solubility in 25 % acetic acid (non-North African samples: 49 ± 15%, North African samples: 49 ± 6.4%). The differences source dependence of Mn solubility in these aerosols between the two leach types is just one example of how challenging it is to model Mn bioavailability in the North Atlantic. Nevertheless, with the exception of soluble Mn from the acetic acid leach, this TE solubility data supports the general assertion that aerosol TE solubility varies as a function of provenance and/or atmospheric loading (e.g. Baker and Jickells, 2006; Sedwick et al., 2007; Sholkovitz et al., 2009; 2012; Aguilar-Islas et al., 2010; Fishwick et al., 2014; Jickells et al., 2016).

3.3.3. Soluble TEs: UHP water compared to seawater instantaneous leaches

Seawater leaches were conducted on a subset of samples (GA03-2011), to investigate the suitability of seawater as the leach medium in the instantaneous leach. During this study, Fe solubility in seawater was

lower than in UHP water (Fig. 6c). This phenomenon has previously been observed in atmospheric aerosols from the North Atlantic Ocean (Buck et al., 2010). For Fe, only a few samples of North American and Marine provenance conformed to the relationship described by the equation proposed by Buck et al. (2010), with most of our data plotting above the regression line of the Buck et al. (2010) study (Fig. 6c), indicating that our data was relatively more soluble in UHP water compared to seawater than in this earlier study. One possibility is that the higher aerosol Fe loadings we observed during GA03-2011 (this study, maximum = 5650 ng Fe m^{-3}), compared to the A16N-2003 transect (Buck et al. 2010; maximum =1330 ng Fe m^{-3}), resulted in a particle concentration effect (Baker and Jickells, 2006), whereby the relationship between aerosol Fe loading and fractional solubility breaks down because dust on the filter can be a source of soluble Fe but can also scavenge dissolved Fe from the sea water leach solution as it passes through the filter. An alternative explanation for the difference in Fe solubility is that the organic composition of the seawater used as the leach mediums differed between the two studies, given that the link between Fe solubility in seawater and Fe-binding ligand availability is well established (e.g. Rue and Bruland, 1995; Gledhill and Buck, 2012).

Mn is the only TE that has a slope close to unity (0.98; Fig. 6b), suggesting that solubility estimates were not impacted by the choice of leach medium used. This is consistent with other studies that have found that Mn solubility is less sensitive to the choice of leach media, or to aerosol provenance than other TEs (Baker et al., 2006; Jickells et al., 2016). Due to the large variability in the data, there was no significant difference between Mn solubility in UHP water or seawater (32 ± 13 % and 24 ± 17 %, respectively; Fig. S1, and Tables S2 and S3, Supplementary Material). Other TEs that also resulted in similar solubility estimates were Al, Cu, Zn and Cd (Figs 6a, f, g and h). However, the data also had high variance, particularly Al, so caution is urged in interpreting this as a 1:1 relationship. Indeed, an ANOVA indicated that the means of the UHP water and seawater leaches were equal for each element at the 95 % confidence level. When the data is considered by aerosol source, however, there were some source dependent differences between the two leaches for Al (North American, Marine and North African), Fe (North African), Co (Marine), Zn (North African), and Cd (North African). The aerosol populations with significant differences between the means are indicated in the brackets.

For Co and Pb (Figs 6d and h), most of the data falls below the 1:1 line, indicating that they were generally more soluble in seawater than UHP water. In contrast, the opposite trend was observed for Fe and Ni (Figs 6c and e), pointing to differences in the availability of metal binding ligands in the seawater used. A challenge of using seawater as the leach medium is that it is difficult to control for natural variability in its organic composition. Consequently, it is not possible to determine conclusively why

contrasting trends in the fractional solubility of TEs were observed. For this reason, we advocate for the use of UHP water as a common leach medium to facilitate comparisons of solubility resulting from differences in aerosol composition. An additional benefit is the ease of analysis of UHP water compared to seawater. That is not to say that seawater should not be used, but rather that it is difficult to draw direct comparisons between datasets due to potential differences in the composition of the seawater used, which could affect the fractional solubility.

3.4. Aerosol acidity

Numerous laboratory studies have demonstrated a link between atmospheric acid species and Fe solubility (e.g. Spokes and Jickells, 1995; Desboeufs et al., 1999; Meskhidze et al., 2003), and in field studies some degree of correlation between nss-SO_4^{2-} and soluble Fe has been observed for samples collected over the Pacific (e.g. Hand et al, 2004; Buck et al., 2013) and Atlantic Oceans (Johansen et al., 2000). However, in other studies in the Atlantic Ocean (Baker et al., 2006; Buck et al., 2010) no relationship was observed. Similarly, we observed no correlation between the soluble acid species, NO_3^- and nss-SO_4^{2-}, and the percentage of UHP water soluble Fe (r^2 = 0.056 and 0.005, respectively). There was also no significant correlation between the percentage of UHP water soluble Fe and aerosol acidity ([NO_3^-] + 2*[nss-SO_4^{2-}]) for the GA03 samples (r^2 = 0.08; Fig. 7a), which further suggests the dominance of North African mineral aerosol, which does not have a large NO_3^- or nss-SO_4^{2-}component (Baker et al., 2006). As acid species and Fe predominantly reside in different size fractions of aerosols (Schulz et al., 1998; Raes et al., 2000), an inverse relationship or no relationship could be a result of a low degree of internal mixing in the aerosol samples, as opposed to aerosol acidity not exerting any control on Fe solubility (Baker et al., 2006), whereas a positive correlation suggests that aerosol acidity is exerting a control on Fe solubility. Further investigation of the GA03 aerosols, split into their provenance categories, suggests that there was little effect of aerosol acidity on Fe solubility for the North American, Marine or North African samples. The European samples also showed no clear trends between the four, uncorrelated data points. In contrast, the weak positive trend in the GA01 samples (High Latitude dust; r^2 = 0.52; Fig. 7b) could be a kinetic effect resulting from aerosol processing at high altitudes.

During their investigations of the GA03 aerosols, Wozniak et al., (2013) proposed a role for water soluble organic carbon (WSOC) in controlling the solubility of Fe. Desboeufs et al. (2005) also found evidence for a link between total carbon and TE solubility in regions impacted by anthropogenic activity. Thus, both aerosol acidity and organic carbon content are implicated as controls on aerosol Fe solubility, but the relationship is frequently not linear. One explanation for this lack of linearity was proposed recently by Hennigan et al. (2015). They concluded that molar (or mass) ratio techniques are not suitable for

predicting aerosol pH (or acidity), and cautioned against drawing conclusions based on proxy methods (e.g. nss-SO_4^{2-} or NO_3^-). Instead, they recommend that either a thermodynamic modelling approach (constrained by gas and aerosol measurements), or the phase partitioning of NH_3, should be used for predicting aerosol pH. Weber et al. (2016) take this further and argue that the best approach for predicting aerosol pH is the phase partitioning of NH_3. These approaches are beyond the scope of the present study, but should be a consideration for future studies due to the pH-dependency of aerosol TE dissolution, especially given the neutralising influence of NH_3, carbonate mineral phases, and sea salt.

4. Conclusions

In this study, five potential aerosol sources were identified based on air mass back trajectory simulations; i) North African, ii) European, iii) North American, iv) High Latitude, and v) Marine. Of these five categories, the North African aerosols were the most homogeneous in terms of their fractional solubility and elemental mass ratios. In contrast, samples from the most remote locations, the Marine and High Latitude aerosols, were the most heterogeneous. Elemental ratios were presented rather than enrichment factors, as earlier work highlighted that the UCC ratios are not representative of the North African mineral dust end-member.

As TE solubility cannot be directly measured, biogeochemical models require a robust relationship between two or more parameters that can be used to predict TE solubility in order to constrain the bioavailable fraction of TEs. However, in regions of high mineral dust deposition and/or productivity fractional solubility (bioavailability by proxy) we are likely to be underestimate solubility using the instantaneous leach approach. As previously reported, we observed an inverse relationship between TE fractional solubility and aerosol provenance/loading for all leach media (UHP water, filtered seawater, and 25 % acetic acid) investigated, with the exception of Mn. However, the large degree of variability in the data meant that few of these differences were statistically significant. There were also differences in the solubility estimates calculated from the different leaches, with values derived from the 25 % acetic acid leach always highest, by approximately an order of magnitude. Leaches conducted using filtered seawater resulted in the lowest values for TE solubility, except for Pb, which was more soluble in seawater than UHP water. Such differences, serve as a reminder that some degree of standardisation is required for aerosol leach protocols, to facilitate comparisons between different studies. This will be key moving forward if TE solubility is to be accurately parametrised in biogeochemical models. Further work is also required to assess which fraction is accessed by the various leach protocols in order to elucidate links between the soluble and bioavailable fractions.

Data availability

Data is available at BCO-DMO (GA03; www.bco-dmo.org) and LEFE-CYBER (GA01; (www.obsvlfr.fr/proof/php/GEOVIDE/GEOVIDE.php), and on request from the lead author.

Acknowledgements

Many thanks to the captains and crews of the RV Knorr (GA03-2010 and 2011) and NO Pourquoi Pas? (GA01), the chief scientists (GA03 = Bob Anderson, Ed Boyle, Greg Cutter; GA01 = Geraldine Sarthou and Pascale Lherminier), Alex Baker for the loan of the aerosol sampler used on GA01, and Alina Ebling Petroc Shelley, Alex Landing and Sarah Huff for their help running samples. This work was supported by grants to WML (NSF-OCE 0752832, 0929919 and 1132766), and GS (ANR-13-B506-0014 and ANR-12-PDOC-0025-01). RUS was supported by a LabexMER International Postdoctoral Fellowship and CG29 Postdoctoral Fellowship. A portion of this work was performed at the National High Magnetic Field Laboratory, which is supported by National Science Foundation Cooperative Agreement No. DMR-1157490 and the State of Florida. The aerosol digestions for GA01 were undertaken in the geochemistry clean room at Ifremer (Centre de Bretagne). Trace element determination for GA01 was conducted at the Pôle de Spectrométrie Océan at the Institut Universitaire Européen de la Mer with the support and guidance of Claire Bollinger and Marie-Laure Rouget.

References

Achterberg, E. P., Moore, C.M., Henson, S. A., Steigenberger, S., Stohl, A., Eckhardt, S., Avendano, LC., Cassidy, M., Hembury, D., Klar, J.K., Lucas, M.I., Macey, A.I., Marsay, C.M., and, Ryan-Keogh, T.J.: Natural iron fertilization by the Eyjafjallajökull volcanic eruption, Geophys. Res. Lett., 40, 921-926, http://doi.org/10.1002/grl.50221, 2013.

Adams, A. M., Prospero, J.M., and Zhang, C.: CALIPSO-Derived Three-Dimensional Structure of Aerosol over the Atlantic Basin and Adjacent Continents, Journal of Climate, 25, 6862-6879, http://doi.org/10.1175/JCLI-D-11-00672.1, 2012.

Aguilar-Islas, A. M., Wu, J., Rember, R., Johansen, A.M. and Shank, L. M.: Dissolution of aerosol-derived iron in seawater: Leach solution chemistry, aerosol type, and colloidal iron fraction, Marine Chemistry, 120, 25-33., 2010.

Arnalds, O.: Soils of Iceland, Jökull, 58, 409-421, 2004.

Baker, A. R., Adams, C., Bell, T.G., Jickells, T.D., and Ganzeveld, L.: Estimation of atmospheric nutrient inputs to the Atlantic Ocean from 50N to 50S based on large-scale filed sampling: Iron and other dust-

associated elements, Global Biogeochem. Cycles, 27, 755-767, http://doi.org/10.1002gbc.20062, 2013, 2013.

Baker, A. R., and, and Croot, P. L.: Atmospheric and marine controls on aerosol iron solubility in seawater., Marine Chemistry., 120, 4-13, 2010.

Baker, A. R., and Jickells, T.D.: Mineral particle size as a control on aerosol iron solubility., Geophys. Res. Lett., 33, http://doi.org/10.1029/2006GL026557, 2006.

Baker, A. R., Jickells, T. D., Witt, M., and Linge, K. L.: Trends in the solubility of iron, aluminium, manganese and phosphorus in aerosol collected over the Atlantic Ocean, Marine Chemistry, 98, 43-58, 2006.

Baker, A. R., Landing, W.M., Bucciarelli, E., Cheize, M., Fietz, S., Hayes, C.T., Kadko, D., Morton, P.L., Rogan, N., Sarthou, G., Shelley, R.U., Shi, Z., Shiller, A., and, van Hulten, M.M.P.: Trace element and isotope deposition across the air–sea interface: progress and research needs, Philosophical Transactions of the Royal Society A: Mathematical, Physical and Engineering Sciences, 374, http://doi.org/10.1098/rsta.2016.0190, 2016.

Ben-Ami, Y., Koren, I., Rudich, Y., Artaxo, P., Martin, S.T., and Andreae, M.O.: Transport of North African dust from the Bodele depression to the Amazon Basin: a case study, Atmos. Chem. Phys., 10, 7533-7544, http://doi.org/10.5194/acp-10-7533-2010, 2010.

Berger, J. M., Lippiatt, S.M., Lawrence, M.G., and Bruland, K.W.: Application of a chemical leach technique for estimating labile particulate aluminum, iron, and manganese in the Columbia River plume and coastal waters off Oregon and Washington., Journal of Geophysical Research, 113, http://doi.org/10.1029/2007JC004703, 2008.

Bridgestock, L., Rehkämper,M., van de Flierdt,T., Murphy, K., Khondoker, R., Baker, A. R., Chance, R., Strekopytov, S., Humphreys-Williams, E., and Achterberg E.P.: The Cd isotope composition of atmospheric aerosols from the Tropical Atlantic Ocean, Geophys. Res. Lett., 44, 2932-2940, http://doi.org/10.1002/2017GL072748, 2017.

Buck, C. S., Landing, W.M., and Resing, J.: Pacific Ocean aerosols: Deposition and solubility of iron, aluminum, and other trace elements, Marine Chemistry, 157, 117-130, http://dx.doi.org/10.1016/j.marchem.2013.09.005, 2013.

Buck, C. S., Landing, W.M., Resing, J. A., Lebon, G. T.: Aerosol iron and aluminum solubility in the northwest Pacific Ocean: Results from the 2002 IOC cruise, Geochemistry, Geophysics, Geosystems., 7, http://doi.org/10.1029/2005GC000977, 2006.

Buck, C. S., Landing, W.M., Resing, J.A. and Measures, C.I.: The solubility and deposition of aerosol Fe and other trace elements in the North Atlantic Ocean: Observations from the A16N CLIVAR/CO_2 repeat hydrography section., Marine Chemistry., 120, 57-70, 2010.

Bullard, J. E., Baddock, M., Bradwell, T., Crusius, J., Darlington, E., Gaiero, D., Gassó, S., Gisladottir, G., Hodgkins, R., McCulloch, R., McKenna-Neuman, C., Mockford, T., Stewart, H., and, Thorsteinsson,

T.: High-latitude dust in the Earth system, Reviews of Geophysics, 54, 447-485, http://doi.org/10.1002/2016RG000518, 2016.

Cheize, M., Sarthou, G., Croot, P., Bucciarelli, E., Baudoux, A.-C., and Baker, A.: Iron organic speciation determination in rainwater using cathodic stripping voltammetry, Analytica Chimica Acta, 726, 45-54, 2012.

Chueinta, W., Hopke, P. K., and Paatero, P.: Investigation of sources of atmospheric aerosol at urban and suburban residential areas in Thailand by positive matrix factorization, Atmospheric Environment, 34, 3319-3329, http://dx.doi.org/10.1016/S1352-2310(99)00433-1, 2000.

Conway, T. M., and John, S.G.: Quantification of dissolved iron sources to the North Atlantic Ocean, Nature, 511, 212-215, http://doi.org/10.1038/nature13482.

Conway, T.M., Shelley, R.U., Aguilar-Islas, A.M., Landing, W.M., Mahowald, N.M., and John, S.G.: Iron isotopes reveal and important anthropogenic aerosol iron flux to the North Atlantic. Submitted to: Nature Communications.

de Leeuw, G., Guieu, C., Arneth, A., Bellouin, N., Bopp, L., Boyd, P.W., Denier van der Gon, H.A.C., Desboeufs, K.V., Dulac, F., Facchini, M.C., Gantt, B., Langmann, B., Mahowald, N.M., Maranon, E., O'Dowd, C., Olgun, N., Pulido-Villena, E., Rinaldi, M., Stephanou, E.G., and Wagener, T. : Ocean-atmosphere interactions of particles, in: Ocean-atmosphere interactions of gases and particles, edited by: Liss, P. S., and Johnson, M.T., Springer-Verlag, Berlin, 171-245, 2014.

Desboeufs, K. V., Losno, R., Vimeux, F., and Cholbi, S.: The pH-dependent dissolution of wind-transported Saharan dust, Journal of Geophysical Research, 104, 21287-21299, 1999.

Desboeufs, K. V., Sofikitis, A., Losno, R., Colin, J. L. and Ausset, P.: Dissolution and solubility of trace metals from natural and anthropogenic aerosol particulate matter., Chemosphere, 58, 195-203., 2005.

Doherty, O. M., Riemer, N., and Hameed, S.: Role of the convergence zone over West Africa in controlling Saharan mineral dust load and transport in the boreal summer, Tellus B, 66, http://doi.org/10.3402/tellusb.v66.23191, 2014.

Fishwick, M. P., Sedwick, P.N., Lohan, M.C., Worsfold, P.J., Buck, K.N., Church, T.M., and Ussher, S.J.: The impact of changing surface ocean conditions on the dissolution of aerosol iron, Global Biogeochem. Cycles, 28, 1235-1250, http://doi.org/10.1002/2014GB 004921, 2014.

Gelado-Caballero, M. D., López-García, P., Prieto, S., Patey, M.D., Collado, C., Hérnández-Brito, J.J.: Long-term aerosol measurements in Gran Canaria, Canary Islands: Particle concentration, sources and elemental composition, Journal of Geophysical Research: Atmospheres, 117, D03304, http://doi.org/10.1029/2011jd016646, 2012.

Gledhill, M., and Buck, K. N.: The organic complexation of iron in the marine environment: a review, Frontiers in Microbiology, https://doi.org/10.3389/fmicb.2012.00069, 2012.

Hand, J. L., Mahowald, N. M., Chen, Y., Siefert, R. L., Luo, C., Subramaniam, A., and Fung, I.: Estimates of atmospheric-processed soluble iron from observations and a global mineral aerosol model:

Biogeochemical implications, Journal of Geophysical Research: Atmospheres, 109, D17205, http://doi.org/10.1029/2004jd004574, 2004.

Hatta, M., Measures, C. I., Wu, J., Roshan, S., Fitzsimmons, J. N., Sedwick, P., and, and Morton, P.: An overview of dissolved Fe and Mn Distributions during the 2010–2011 U.S. GEOTRACES north Atlantic Cruises: GEOTRACES GA03, Deep Sea Research Part II: Topical Studies in Oceanography, http://dx.doi.org/10.1016/j.dsr2.2014.07.005, 2015.

Helmers, E., and Schrems, O.: Wet deposition of metals to the tropical North and the South Atlantic Ocean, Atmospheric Environment, 29, 2475-2484, 1995.

Hennigan, C. J., Izumi, J., Sullivan, A. P., Weber, R. J., and Nenes, A.: A critical evaluation of proxy methods used to estimate the acidity of atmospheric particles, Atmos. Chem. Phys., 15, 2775-2790, http://doi.org/10.5194/acp-15-2775-2015, 2015.

Jickells, T. D., Baker, A. R., and Chance, R.: Atmospheric transport of trace elements and nutrients to the oceans, Philosophical Transactions of the Royal Society A: Mathematical, Physical and Engineering Sciences, 374, http://doi.org/10.1098/rsta.2015.0286, 2016.

Jickells, T. D., An, Z.S., Andersen, K.K., Baker, A.R., Bergametti, G., Brooks, N., Cao, J.J., Boyd, P.W., Duce, R.A., Hunter, K.A., Kawahata, H., Kubilay, N., laRoche, J., Liss, P.J., Mahowald, N., Prospero, J.M., Ridgwell, A.J., Tegen, I., and Torres, R.: Global iron connections between desert dust, ocean biogeochemistry and climate., Science, 308, 67-71, 2005.

Johansen, A., Siefert, R.L., Hoffmann, M.R.: Chemical composition of aerosols collected over the tropical North Atlantic Ocean, Journal of Geophysical Research, 105, 15277-15312, 2000.

Kim, G., Alleman, L.Y., and Church, T.M.: Atmospheric depositional fluxes of trace elements, 210Pb, and 7Be to the Sargasso Sea, Global Biogeochemical Cycles, 13, http://doi.org/1183-1192, 10.1029/1999gb900071, 1999.

Koçak, M., Kubilay, N., Herut, B., and Nimmo, M.: Trace Metal Solid State Speciation in Aerosols of the Northern Levantine Basin, East Mediterranean, Journal of Atmospheric Chemistry, 56, 239-257, http://doi.org/10.1007/s10874-006-9053-7, 2007.

Laing, J. R., Hopke, P.K., Hopke, E.F., Husain, L., Dutkiewicz, V.A., Paatero, J., and Viisanen, Y.: Positive Matrix Factorization of 47 Years of Particle Measurements in Finnish Arctic, Aerosol and Air Quality Research, 15, 188-207, http://doi.org/10.4209/aaqr.2014.04.0084, 2015.

Landing, W.M., and Shelley, R.U.: Particle size effects on aerosol iron solubility from the U.S. GEOTRACES North Atlantic Zonal Transect (2010, 2011), ASLO 2013 Aquatic Sciences Meeting, 2013.

Longhurst, A.: Ecological Geography of the Sea., Academic Press., San Diego, 1998.

Longo, A. F., Feng, Y., Lai, B., Landing, W.M., Shelley, R.U., Nenes, A., Mihalopoulos, N., Violaki, K., and, Ingall, E.D.: Influence of Atmospheric Processes on the Solubility and Composition of Iron in Saharan Dust, Environmental Science & Technology, 50, 6912-6920, http://doi.org/10.1021/acs.est.6b02605, 2016.

690 Mackey, K. R. M., Chien, C.-T., Post, A.F., Saito, M.A., and Paytan, A.: Rapid and gradual modes of
691 aerosol trace metal dissolution in seawater, Frontiers in Microbiology, 5, 1-11,
692 http://doi.org/10.3389/fmicb.2014.00794, 2015.

693 Maring, H., Settle, D.M., Buat-Ménard, P., Dulac, F., and, Patterson, C.C.: Stable lead isotopes tracers of
694 air mass trajectories in the Mediterranean region, Nature, 300, 154-156, 1987.

695 Measures, C.I., and Brown E.T.: Estimating dust input to the Atlantic Ocean using surface water Al
696 concentrations, in, The Impact of desert dust across the Mediterranean, edited by S. Guerzoni and R.
697 Chester, pp.301-311, Kluwer: Dordrecht, 1996.

698 Meskhidze, N., Chameides, W. L., Nenes, A., and Chen, G.: Iron mobilization in mineral dust: Can
699 anthropogenic SO_2 emissions affect ocean productivity? Geophysical Research Letters, 30, 2085,
700 http://doi.org/10.1029/2003gl018035, 2003.

701 Morton, P. L., Landing, W.M.,Hsu, S.-C., Milne, A., Aguilar-Islas, A.M., Baker, A.R., Bowie, A.R.,
702 Buck, C.S., Gao, Y., Gichuki, S., Hastings, M.G., Hatta, M., Johansen, A. M., Losno, R., Mead, C.,
703 Patey, M.D., Swarr, G., Vandermark, A., Zamora, L.M.: Methods for the sampling and analysis of marine
704 aerosols: results from the 2008 GEOTRACES aerosol intercalibration experiment, Limnology and
705 Oceanography: Methods, 11, 62-78, 2013.

706 Paris, R., Desboeufs, K.V., and Journet, E.: Variability of dust iron solubility in atmospheric waters:
707 Investigation of the role of oxalate organic complexation, Atmospheric Environment, 45, 6510-6517,
708 http://dx.doi.org/10.1016/j.atmosenv.2011.08.068, 2011.

709 Patey, M. D., Achterberg, E.P., Rijkenberg, M.J., and Pearce, R.: Aerosol time-series measurements over
710 the tropical Northeast Atlantic Ocean: Dust sources, elemental, composition and mineralogy, Marine
711 Chemistry, 174, 103-119, http://dx.doi.org/10.1016/j.marchem.2015.06.004, 2015.

712 Powell, C. F., Baker, A.R., Jickells, T.D., Bange, H.W., Chance, R.J., Yodle, C.: Estimation of the
713 atmospheric flux of nutrients and trace metals to the eastern tropical North Atlantic Ocean, Journal of the
714 Atmospheric Sciences, 4029-4045, http://doi.org/10.1175/JAS-D-15-0011.1, 2015.

715 Prospero, J. M., Bullard, J.E., and Hodgkins, R.: High-Latitude Dust Over the North Atlantic: Inputs from
716 Icelandic Proglacial Dust Storms, Science, 335, 1078-1082, http://doi.org/10.1126/science.1217447,
717 2012.

718 Prospero, J. M., Glaccum, R.A. and Nees, R.T.: Atmospheric transport of soil dust from Africa to South
719 America., Nature., 289, 570-572., 570-572., 1981.

720 Raes, F., Van Dingenen, R., Vignati, E., Wilson, J., Putaud, J.-P., Seinfeld, J. H., and Adams, P.:
721 Formation and cycling of aerosols in the global troposphere, Atmospheric Environment, 34, 4215-4240,
722 2000.

723 Rolph, G.D., Real-time Environmental Applications and Display sYstem (READY) Website
724 (http://ready.arl.noaa.gov). NOAA Air Resources Laboratory, Silver Spring, MD, 2017.Rubin, M.,
725 Berman-Frank, I., and Shaked, Y.: Dust- and mineral-iron utilization by the marine dinitrogen-fixer
726 Trichodesmium, Nature Geosci, 4, 529-534, 2011.

Rudnick, R. L., and Gao, S.: Composition of the continental crust, in: Treatise on Geochemistry, edited by: Holland, H. D., and Turekian, K.K., Elsevier, Oxford, 1-64, http://dx.doi.org/10.1016/B0-08-043751-6/03016-42003.

Rue, E. L., and Bruland, K. W. : Complexation of iron (III) by natural organic ligands in the Central North Pacific as determined by a new competiative ligand equilibrium/ adsorptive cathodic stripping voltammetric method, Marine Chemistry, 50, 117-138, 1995.

Sarthou, G., Baker, A.R., Blain, S., Achterberg, E.P., Boye, M., Bowie, A.R., Croot, P., Laan, P., de Baar, H.J. W., Jickells, T.D. and Worsfold, P.J.: Atmospheric iron deposition and sea-surface dissolved iron concentrations in the eastern Atlantic Ocean., Deep Sea Research Part I: Oceanographic Research Papers., 50, 1339-1352., 2003.

Scheuvens, D., Schütz, L., Kandler, K., Ebert, M., and Weinbruch, S.: Bulk composition of northern African dust and its source sediments — A compilation, Earth-Science Reviews, 116, 170-194, http://dx.doi.org/10.1016/j.earscirev.2012.08.005, 2013.

Schmidt, K., Schlosser, C., Atkinson, A., Fielding, S., Venables, H.J., Waluda, C.M., and Achterberg, E.P.: Zooplankton gut passage mobilizes lithogenic iron for ocean productivity, Current Biology, 26, 2667-2673, https://doi.org/10.1016/j.cub.2016.07.058, 2016.

Schulz, M., Balkanski, Y.J., Guelle, W., Dulac, F. : Role of aerosol size distribution and source location in a three-dimensional simulation of a Saharan dust episode tested against satellite-derived optical thickness, Journal of Geophysical Research, 103, 10579–10592, 1998.

Sedwick, P. N., Sholkovitz, E.R. and Church, T.M.: Impact of anthropogenic combustion emissions on the fractional solubility of aerosol iron: evidence from the Sargasso Sea., Geochemistry, Geophysics, Geosystems., 8, http://doi.org/10.1029/2007GC001586, 2007.

Shaked, Y., and Lis, H.: Dissassembling iron availability to phytoplankton, Frontiers in Microbiology, 3, http://doi.org/10.3389/fmicb.2012.00123, 2012.

Shelley, R. U., Morton, P.L. and Landing, W.M.: Elemental ratios and enrichment factors in aerosols from the US-GEOTRACES North Atlantic transects, Deep Sea Research Part II: Topical Studies in Oceanography, 116, 262-272, http://dx.doi.org/10.1016/j.dsr2.2014.12.005, 2015.

Shelley, R. U., Roca-Martí, M., Castrillejo, M., Sanial, V., Masqué, P., Landing, W.M., van Beek, P., Planquette, H., and, Sarthou, G.: Quantification of trace element atmospheric deposition fluxes to the Atlantic Ocean (> 40°N; GEOVIDE, GEOTRACES GA01) during spring 2014, Deep Sea Research Part I: Oceanographic Research Papers, 119, 34-49, http://doi.org/10.1016/j.dsr.2016.11.010, 2017.

Sholkovitz, E., R., Sedwick, P.N. and Church, T.M.: Influence of anthropogenic combustion emissions on the deposition of soluble aerosol iron to the ocean: Empirical estimates for island sites in the North Atlantic., Geochimica et Cosmochimica Acta., 73, 3981-4003., 2009.

Sholkovitz, E., R., Sedwick, P.N., Church, T.M., Baker, A.R., and Powell, C.F.: Fractional solubility of aerosol iron: Synthesis of a global-scale data set, Geochimica et Cosmochimica Acta, 89, 173-189, 2012.

Skonieczny, C., Bory, A. Bout-Roumazeilles, V., Abouchami, W., Galer, S. J. G., Crosta, X. Stuut, J.-B., I. Meyer, Chiapello, I., Podvin, T., Chatenet, B., Diallo, A., and Ndiaye, T.: The 7–13 March 2006 major

765 Saharan outbreak: Multiproxy characterization of mineral dust deposited on the West African margin,
766 Journal of Geophysical Research, 116, http://doi.org/10.1029/2011JD016173, 2011.

767 Solmon, F., Chuang, P. Y., Meskhidze, N., and Chen, Y.: Acidic processing of mineral dust iron by
768 anthropogenic compounds over the north Pacific Ocean, J. Geophys. Res., 114, D02305,
769 http://doi.org/10.1029/2008jd010417, 2009.

770 Spokes, L., and Jickells, T.: Factors controlling the solubility of aerosol trace metals in the atmosphere
771 and on mixing into seawater, Aquat Geochem, 1, 355-374, http://doi.org/10.1007/BF00702739, 1995.

772 Stein, A.F., Draxler, R.R, Rolph, G.D., Stunder, B.J.B., Cohen, M.D., and Ngan, F.: NOAA's HYSPLIT
773 atmospheric transport and dispersion modeling system, Bull. Amer. Meteor. Soc., 96, 2059-2077,
774 http://doi.org/10.1175/BAMS-D-14-00110.1, 2015.

775 Ussher, S. J., Achterberg, E.P., Powell, C., Baker, A.R., Jickells, T.D., Torres, R., and Worsfold, P.J.:
776 Impact of atmospheric deposition on the contrasting iron biogeochemistry of the North and South Atlantic
777 Ocean, Global Biogeochemical Cycles, 27, 1096-1107, http://doi.org/10.1002/gbc.20056, 2013.

778 Weber, R. J., Guo, H., Russell, A.G., and Nenes, A.: High aerosol acidity despite declining atmospheric
779 sulfate concentrations over the past 15 years, Nature Geosci, 9, 282-285, http://doi.org/10.1038/ngeo2665

780 Wozniak, A. S., Shelley, R.U., McElhenie, S.D., Landing, W.M., and Hatcher, P.G.: Aerosol water
781 soluble organic matter characteristics over the North Atlantic Ocean: Implications for iron-binding ligands
782 and iron solubility, Marine Chemistry, 173, 162-172, http://dx.doi.org/10.1016/j.marchem.2014.11.002,
783 2014.

784 Wozniak, A. S., Shelley, R.U., Sleighter, R.L., Abdulla, H.A.N., Morton, P.L., Landing, W.M., and
785 Hatcher, P.G.: Relationships among aerosol water soluble organic matter, iron and aluminum in
786 European, North African, and Marine air masses from the 2010 US GEOTRACES cruise, Marine
787 Chemistry, 154, 24-33, http://dx.doi.org/10.1016/j.marchem.2013.04.011, 2013.

788
789

790

791

792

Biogeosciences Discuss., https://doi.org/10.5194/bg-2017-415
Manuscript under review for journal Biogeosciences
Discussion started: 1 November 2017

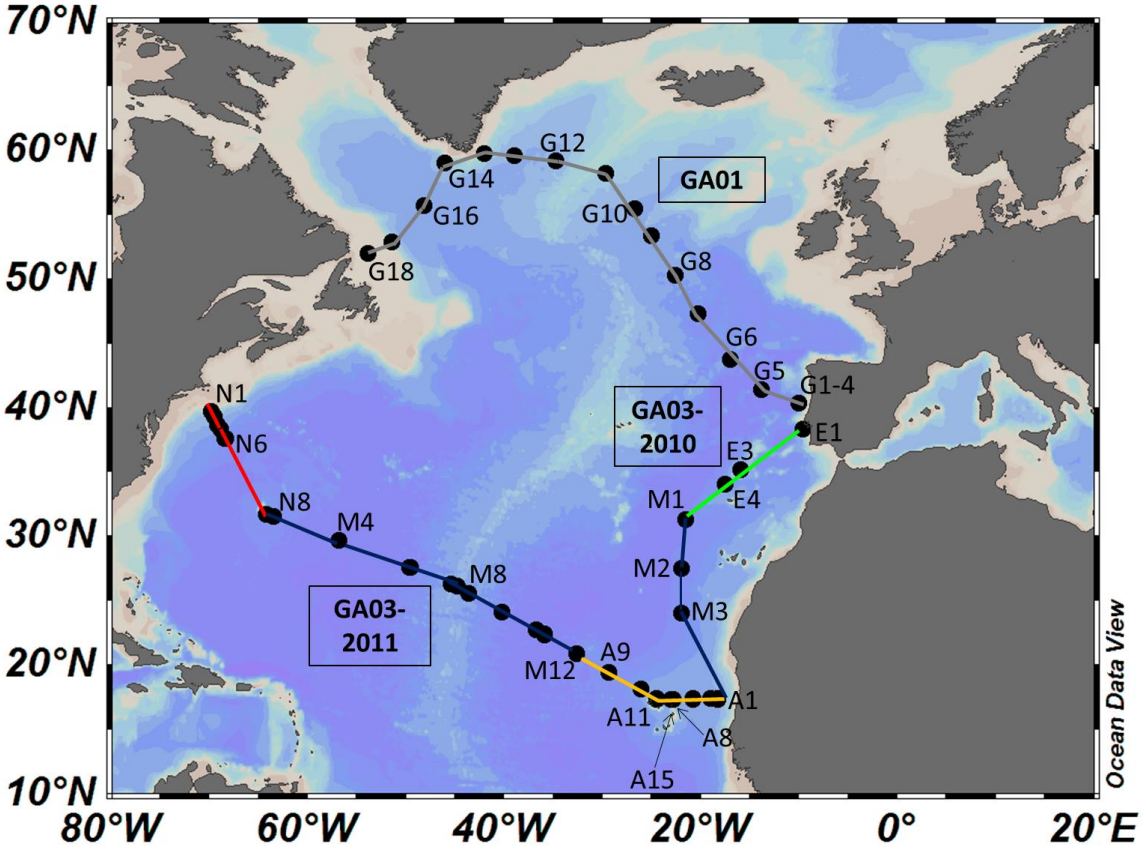

793

794 **Figure 1**

795
796
797
798
799

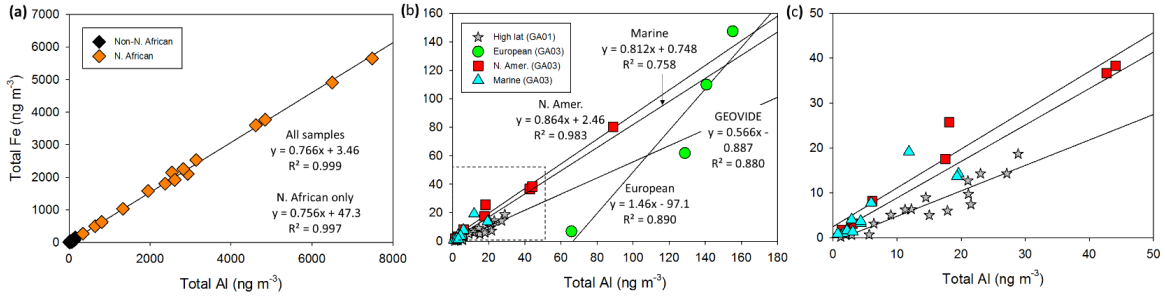

800

801 **Figure 2**

802
803

Biogeosciences Discuss., https://doi.org/10.5194/bg-2017-415
Manuscript under review for journal Biogeosciences
Discussion started: 1 November 2017

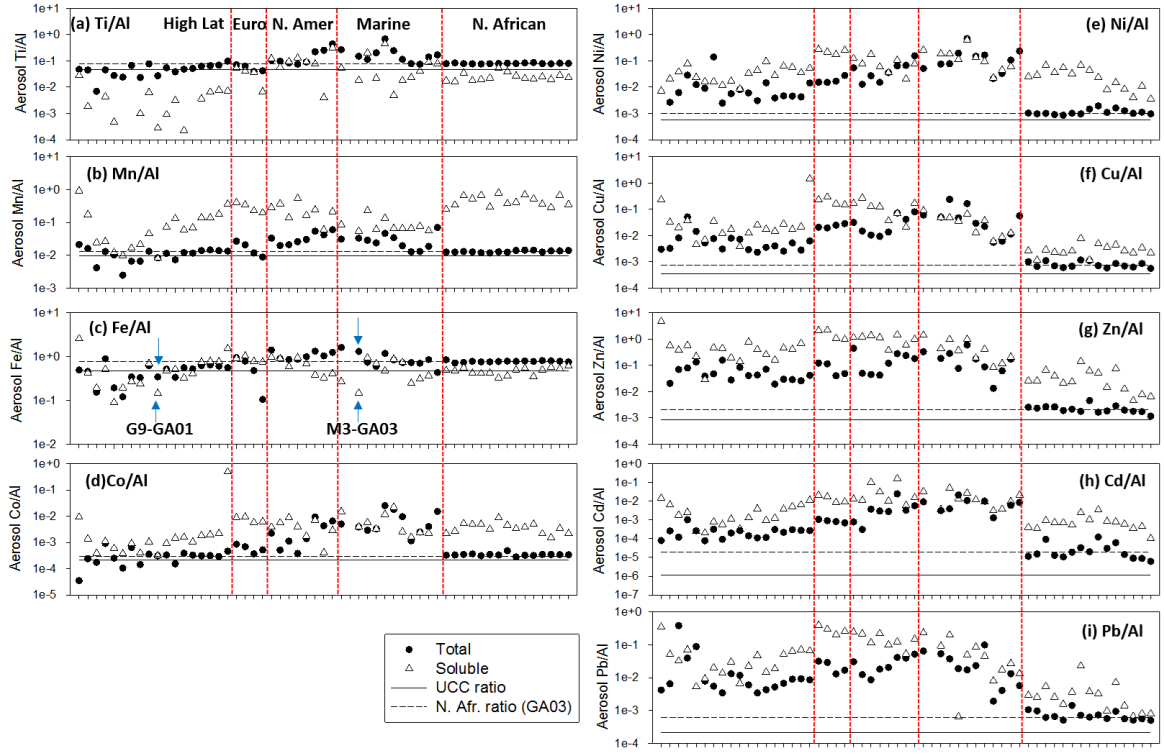

Figure 3

Biogeosciences Discuss., https://doi.org/10.5194/bg-2017-415
Manuscript under review for journal Biogeosciences
Discussion started: 1 November 2017

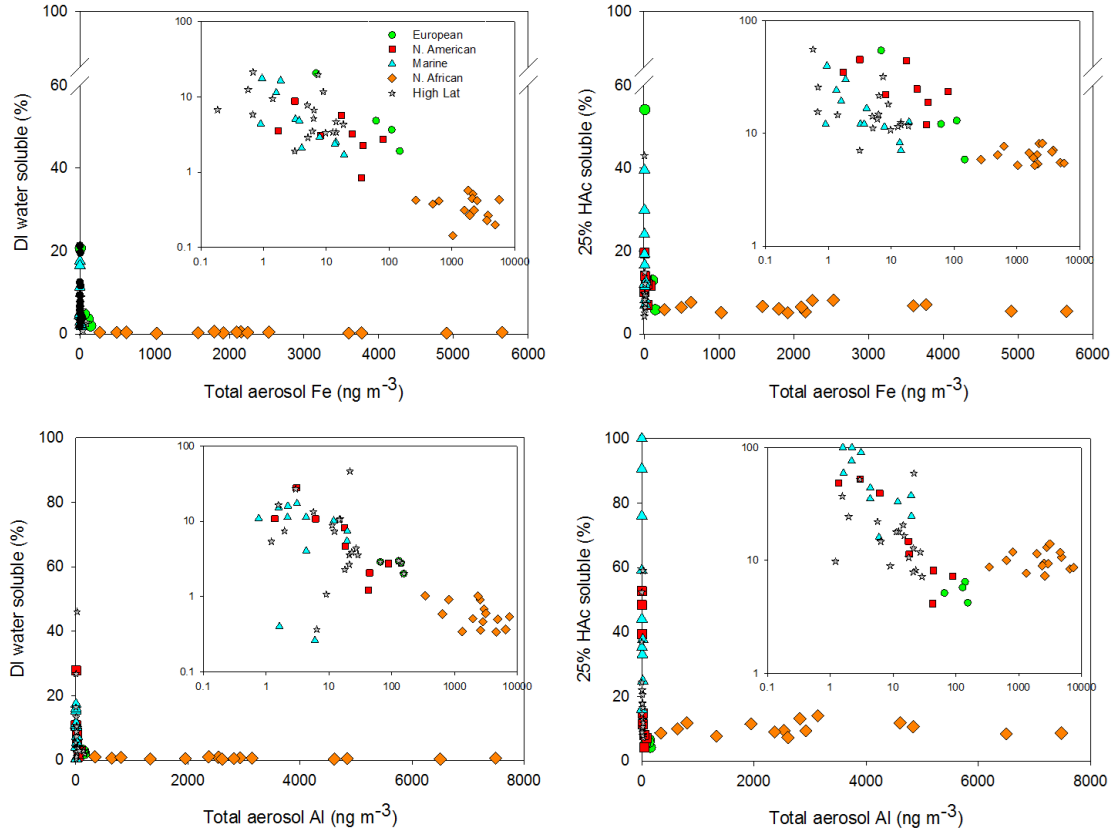

Figure 4

Biogeosciences Discuss., https://doi.org/10.5194/bg-2017-415
Manuscript under review for journal Biogeosciences
Discussion started: 1 November 2017

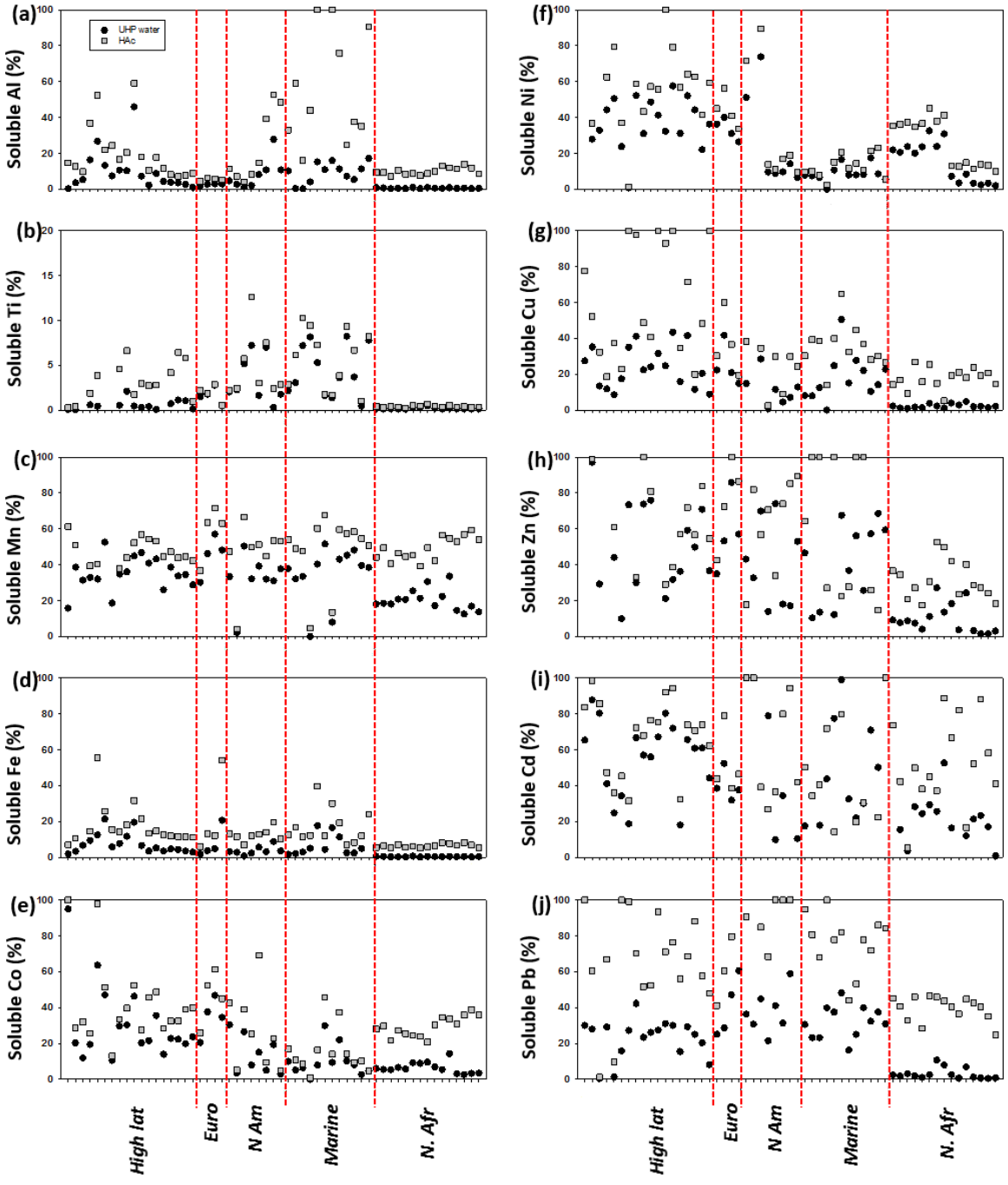

Figure 5

Biogeosciences Discuss., https://doi.org/10.5194/bg-2017-415
Manuscript under review for journal Biogeosciences
Discussion started: 1 November 2017

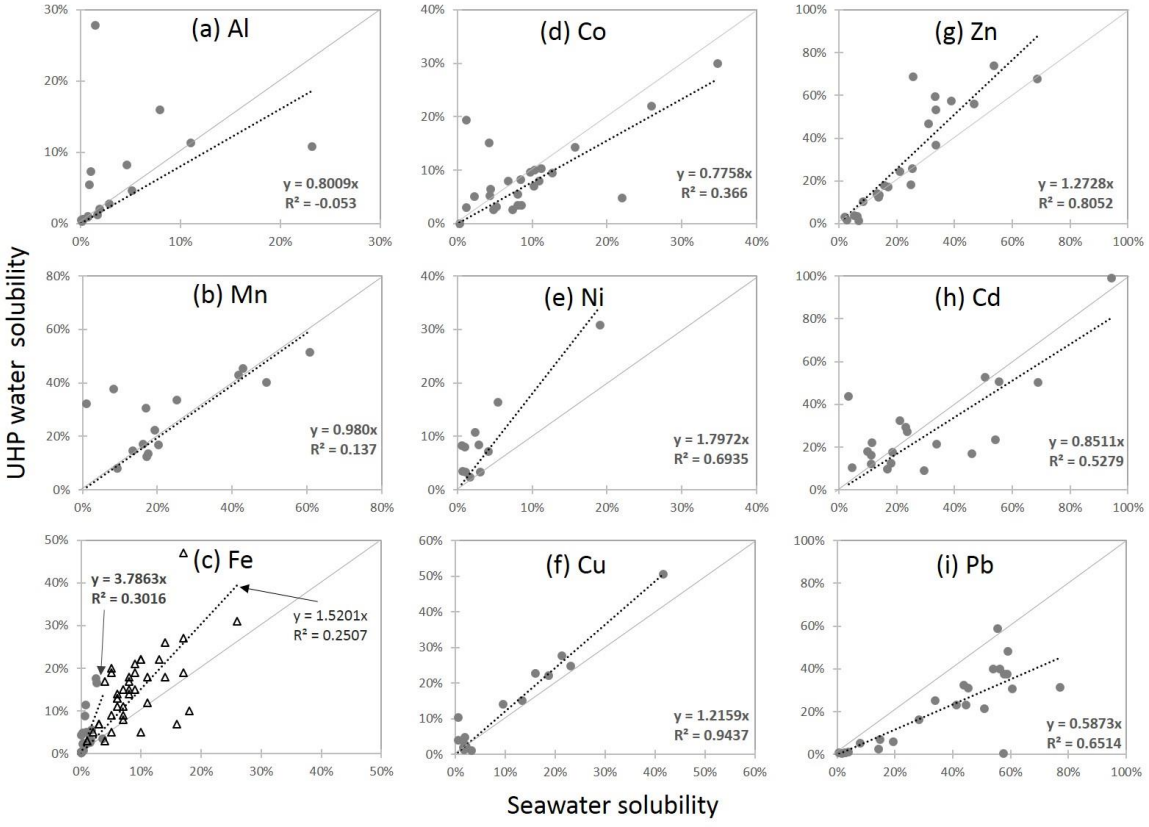

Figure 6

Biogeosciences Discuss., https://doi.org/10.5194/bg-2017-415
Manuscript under review for journal Biogeosciences
Discussion started: 1 November 2017

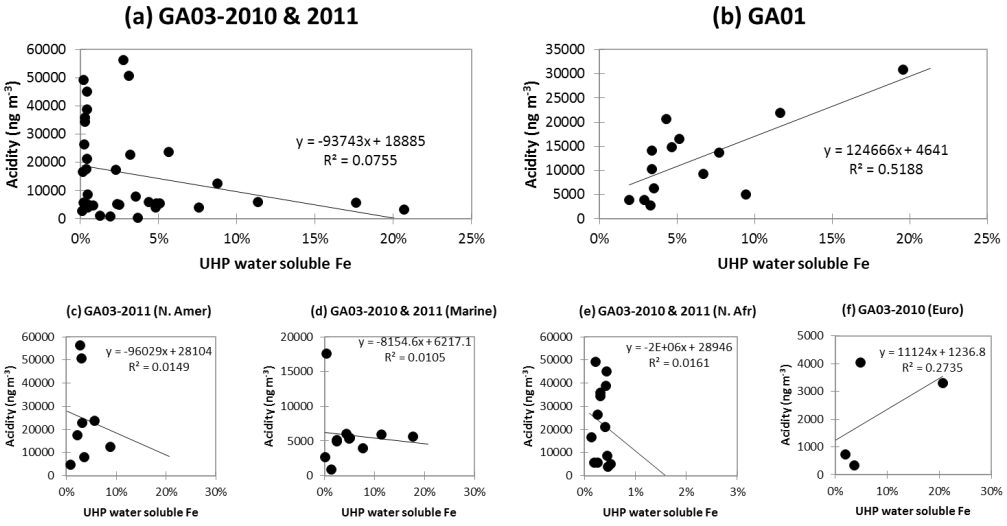

Figure 7

Captions

Figure 1. The GEOTRACES GA01 and GA03 cruise tracks (GA01, GA03-2010 and GA03-2011). In total, 57 aerosol samples (GA01 n = 18, GA03 n = 39; black dots) were collected. The samples are grouped by aerosol provenance (green = European (E1-4), blue = Marine (M1-12), yellow = North African (A1-15), red = North American (N1-8), and grey = High Latitude (G1-18)), identified from air mass back trajectory simulations using the NOAA ARL model, HYSPLIT (Stein et al., 2015; Rolph, 2017).

Figure 2. Total aerosol Fe and Al (ng m^{-3}) for: (a) all aerosol samples from cruises GA01 and GA03, (b) samples from sources other than North Africa (i.e. the black diamonds in Fig. 2a), and (c) the samples inside the dashed box in Fig. 2b. For High Latitude dust n = 18, European samples n = 4, North American samples n = 8, Marine samples n = 12, and Saharan samples n = 15.

Figure 3. Elemental mass ratios (normalised to Al) of total (black circles) and UHP water soluble (white triangles) TEs. The UCC elemental ratio (Rudnick and Gao, 2003) is indicated by the solid horizontal line, and the elemental ratio in North African sourced aerosols (Shelley et al., 2015) is indicated by the dashed horizontal line on each plot. The red vertical lines separate the aerosol source regions, which are labelled in panel (a). Samples G9-GA01 and M3-GA03 are indicated by blue arrows in panel c (see text for details).

Figure 4. (a) Percentage of UHP water soluble Fe versus total aerosol Fe (ng m^{-3}), (b) percentage of 25 % acetic acid soluble Fe versus total aerosol Fe (ng m^{-3}), (c) percentage of UHP water soluble Al versus total aerosol Al (ng m^{-3}), and (d) percentage of 25 % acetic acid soluble Al versus total aerosol Al (ng m^{-3}). the percentage of soluble Fe, or Al, versus total Fe, or Al, is described by a hyperbolic function (Sholkovitz et al., 2009; 2012). The insets in each panel plot the same data on log-log scales to demonstrate the inverse relationship between the two parameters.

Figure 5. Solubility of Al, Ti, Mn, Fe, Co, Ni, Cu, Zn, Cd, Pb following a UHP water leach (UHP water, black circles), and a sequential leach of 25 % acetic acid (HAc, grey squares). The red vertical dashed lines represent the different aerosol source categories, as labelled in panel (b). Note that Ti (panel b) is highly insoluble and the y axis has a maximum value of 20%.

Figure 6. Comparison of TE solubility following instantaneous leaches using UHP water or locally-collected, filtered seawater. The solid line is the 1:1 line. Where fewer data are observed, concentrations were below detection for one or both of the two leaches. The data from Buck et al. (2010) is plotted as open triangles in panel (c).

Figure 7. Aerosol acidity versus UHP water soluble Fe (%) for (a) GA03-2010 and 2011, (b) GA01 – High Latitude dust, (c) GA03 – N. American, (d) GA03 – Marine, (e) GA03 – North African, and (f) GA03 – European samples.